Research Article | Vol. 24, No. 15 / 25 Jul 2016 / OPTICS EXPRESS 16410

Optics EXPRESS

Almost-total absorption of light in thin, biperiodic, weakly-absorbing semiconductor gratings

EVGENY POPOV,[1] ANNE-LAURE FEHREMBACH[1] AND ROSS C. MCPHEDRAN[2,*]

[1]*Aix-Marseille Université, CNRS, Ecole Centrale Marseille, Institut Fresnel UMR 7249, 13013 Marseille, France*

[2]*CUDOS and IPOS, School of Physics, University of Sydney, Sydney, 2006, Australia*

[*]*ross@physics.usyd.edu.au*

Abstract: We consider the design of optical systems capable of providing near 100% absorption of visible light, consisting of a structured thin layer of a weakly absorbing semiconductor placed on top of a dielectric spacer layer and a metallic mirror layer. We generalise a system recently studied semi-analytically and experimentally by Stürmberg *et al* [Optica **3**, 556 2016] which incorporated a grating layer of antimony sulphide and delivered high, narrow-band absorptance of normally-incident light for a single polarisation. We demonstrate that bi-periodic gratings can be optimised to deliver near–perfect absorptance of unpolarised light in the system, and comment on the wavelength and angular ranges over which the absorptance remains near 100%. We show that the properties of the systems studied depend on the interaction of multiple modes, and cannot be accurately modelled within the quasistatic approximation.

OCIS codes: (050.1950) Diffraction gratings; (130.7408) Wavelength filtering devices; (310.3915) Metallic, opaque, and absorbing coatings; (310.6628) Subwavelength structures, nanostructures.

References and links

1. L. M. Hadley and D. M. Dennison, "Reflection and Transmission Interference Filters," J. Opt. Soc. Amer. **37**, 451–465 (1947) .
2. L.C. Botten, R. C. McPhedran, N.A. Nicorovici and G.H. Derrick, "Periodic Models for Thin Optimal Absorbers of Electromagnetic Radiation," Phys. Rev. B **55**, R10672–R10682 (1997).
3. C.A. Davis, D. R. McKenzie and R.C. McKenzie, "Optical Properties and Microstructure of Thin Silver Films," Opt. Commun. **85**, 70–82 (1991).
4. M. C. Hutley and D. Maystre, "The total absorption of light by a diffraction grating," Opt. Commun. **19**, 431–436 (1976).
5. E. Popov, D. Maystre, R.C. McPhedran, M. Nevière, M.C. Hutley, and G.H Derrick, "Total absorption of unpolarised light by crossed gratings," Opt. Express **16**, 6146–6155 (2008).
6. W.W. Salisbury, "Absorbent body for electromagnetic waves," U.S. Patent 2599944, June 10, 1952.
7. Y.D. Chong, L.Ge, H. Cao and A.D. Stone, "Coherent perfect absorbers: Time-reversed lasers," Phys. Rev. Lett. **105**, 1–4 (2010).
8. J. A. Giese, J. W. Yoon, B. R. Wenner, J. W. Allen, M. S. Allen, and R. Magnusson, "Guided-mode resonant coherent light absorbers," Opt. Lett. **39**, 486–488 (2014).
9. A. L. Fannin, J. W. Yoon, B. R. Wenner, J. W. Allen, M. S. Allen and R. Magnusson, "Experimental Evidence for Coherent Perfect Absorption in Guided-Mode Resonant Silicon Films," IEEE Photon. J. **8**, 6802307 (2016).
10. M.A. Kats, "Ultra-thin perfect absorber employing a tunable phase change material," Appl. Phys. Lett. **101**, 221101 (2012).
11. J.R. Piper and S. Fan, "Total Absorption in a Graphene Monolayer in the Optical Regime by Critical Coupling with a Photonic Crystal Guided Resonance," ACS Photonics **1**, 343–353 (2014).
12. Q-C Zhang and D.R. Mills, "Very-low emittance solar selective surfaces using new film structures," J. Appl. Phys. **72**, 3013–3021.
13. G.H. Derrick, R.C. McPhedran and D. R. McKenzie, "Theoretical studies of textured amorphous silicon solar cells," Appl. Opt. **25**, 3690–3696 (2012).
14. W.T. Perrins, D.R. McKenzie and R.C. McPhedran, "Transport Properties of Regular Arrays of Cylinders," Proc. R. Soc. Lond. A **369**, 207–225 (1979).
15. B.C.P. Stürmberg, T.K. Chong, D-Y Choi, T.P. White, L.C. Botten, K.B. Dossou, C. G. Poulton, K.R. Catchpole, R.C. McPhedran and C. M. de Sterke, "Total absorption of visible light in ultrathin weakly absorbing semiconductor

#262839 http://dx.doi.org/10.1364/OE.24.016410
Journal © 2016 Received 12 Apr 2016; revised 4 Jun 2016; accepted 22 Jun 2016; published 12 Jul 2016

Optics EXPRESS

gratings," Optica **3**, 556–562 (2016).
16. B.J. Eggleton, B. Luther-Davies and K. Richardson, "Chalcogenide photonics," Nature Photonics **5**, 141–148 (2011).
17. L. Li, "Use of Fourier series in the analysis of discontinuous periodic structures," J. Opt. Soc. Am. A **13**, 1870–1876 (1996)
18. L.Li, "New formulation of the Fourier modal method for crossed surface relief gratings," J. Opt. Soc. Am. A **14**, 2758–2767 (1997).
19. M. Nevière and E. Popov, "Crossed gratings," in *Light Propagation in Periodic Media, Differential Theory and Design* (Marcel Dekker, New York, 2003), Chap. 9.

1. Introduction

The question of how to create an optical structure which is as black as possible, i.e. which reflects the smallest amount of incident light is one which has long fascinated scientists, technologists and even artists. The answer to the question depends upon what constraints are placed on the structure- whether it is required to be thin or can be thick compared with the wavelength, whether it is required to cover the visible spectrum, or can be narrowband, whether it must work over a wide range of incident angles or not, and whether it must work for polarised or unpolarised light.

Some definitive statements can be made however. If the absorbing structure is required to be much thinner than the incident wavelength and is up-down symmetric (precluding the incorporation of a mirror in the system), then the maximum absorptance it can have is 50% [1, 2] . The argument underlying this result relies on the wavelength being long enough compared with the period of the structure that fields within it can be represented in terms of a superposition of a symmetric and an anti-symmetric mode, with only one of the two able to contribute significantly to the absorption. Surprisingly enough, it is not difficult to make an thin absorber (8-10 nm thick) which comes close to delivering this optimal absorptance over a very wide wavelength range (1.5 μm to at least 43 μm) [3]. If the absorbing structure is allowed to be thick, then 100% absorptance is possible, for example using plasmonic resonance for a single polarisation using a metallic grating [4] or using a biperiodic metallic grating for unpolarised light, with the grating parameters chosen to ensure plasmon resonances for two orthogonal polarisations at the same wavelength [5]. A second method to deliver 100% absorptance is to place a perfectly reflecting mirror behind a thin absorbing layer, at the appropriate distance with respect to the wavelength to make the incoming waves from above and below interfere in phase at the layer. This is the Salisbury configuration [6], with the associated mechanism sometimes being called coherent perfect absorption [7–10].The design principle associated with this configuration is referred to as critical coupling [11]: the system is required to satisfy the property that the absorption of the layer exactly balances the rate of delivery of energy to it. The separation between the mirror and the thin layer is a critical parameter of this method, and the bandwidth of strong absorption it can deliver is generally narrow in consequence.

There is an extensive literature on the design of structured systems to achieve high absorptance over either a narrow or a controlled spectral range. For example, in the development of photothermal absorbing systems for alternative energy applications, composite material systems composed of metallic particles mixed in a ceramic matrix have been designed and fabricated, and show high absorptance for wavelengths up to 1.5 μm, switching to high reflectance at longer wavelengths [12]. For photovoltaic cells, the design requirements combine optical absorption characteristics with electronic properties, necessitating use of different materials from those prevalent in photothermal applications. Texturing has long been employed in this latter application to reduce front-surface reflection losses and help maximise absorption in layers as thin as possible. While singly-periodic texture profiles are often studied and have been shown to strongly improve cell performance for a chosen polarisation of incident light, it is often desirable to employ doubly-periodic texturing, which can deliver high polarisation-independent absorptance. For an early example of a theoretical study of this less-studied effect of doubly-periodic texturing,

Optics EXPRESS

see the investigation of thin photovoltaic cells consisting of indium-tin oxide front layers and amorphous hydrogenated silicon absorbing layers on silver substrates [13]. The photovoltaic application favours the use of semiconductors for light absorption, and it is desirable that the materials used be compatible with CMOS fabrication.

While rigorous electromagnetic codes are typically used in simulations of structured absorbing systems, it is sometimes the case that designs may be conceived on the basis of simple effective medium approaches. These typically work best when the wavelength is much larger than the scale size of the structuring, but the domain of applicability of course depends on the strength of the contrast between the permeabilities or permittivities of the materials in use, with lower contrasts favouring the use of effective medium formulae for wavelengths close to the scale size. We will use here effective medium formulae [14] specifically derived for square and triangular lattices of cylinders, and incorporating terms up to the twelfth power of volume fraction, rather than the second order accuracy of the usual Maxwell-Garnett theory. We will show that the resonant absorption effects given by rigorous codes show details and even gross effects which are not predicted by the effective medium formulae for the geometries and materials studied here.

In a recent paper, Stürmberg *et al* considered the weakly absorbing semiconductor material antimony sulphide, and showed that thin layer $\sim \lambda/15$of it could be incorporated into a system with a silica spacer and a silver reflecting layer in such a way as to deliver total absorption, when an appropriate lamellar grating profile was applied to the antimony sulphide layer. The system was fabricated and had a visible absorptance of 99.3% at $\lambda = 591$nm, in excellent agreement with theory. Of the total absorptance of 99.3%, only 0.6% was due to the silver mirror. The grating structure was singly-periodic, and the high absorptance only occurred in one polarisation of normally-incident light.

It is our aim here to take the same chalcogenide material (antimony sulphide) as Stürmberg *et al* and use a doubly-periodic grating with cylindrical elements rather than a lamellar grating, and investigate the design of systems capable of near-perfect absorption of incident light, for both polarisations simultaneously. We will compare the two isotropic lattice arrangements (square and triangular) appropriate to normal incidence, and determine the angular extent of the low-reflectance regions for each, as well as the effect of the choice as to whether the antimony sulphide is the connected or disconnected phase in the doubly-periodic surface topology, as well as that of the second material used in the doubly-periodic grating structure. Our results indicate that a range of these designs can deliver near perfect absorption, but that the designs do deliver different absorption bandwidths, different proportions of absorption in antimony sulphide and in the mirror as well as different angular sensitivities. The results are important, in that the chalcogenide group furnishes a whole class of valuable CMOS-compatible materials for photonics, with emerging applications in mid-infrared sensing, integrated optics and ultrahigh-bandwidth signal processing [16]. We believe that the results we give here come from the first investigation in the literature of polarisation-insensitive absorption enhancement for thin chalcogenide layers.

2. Numerical studies

In order to generalise the lamellar grating of Stürmberg *et al* [15] to a doubly-periodic grating delivering polarisation-insensitive reflection and absorption for normally incident radiation, we have chosen a structure composed of cylinders arranged in either the square or triangular arrays, with equal spacing along periodicity axes. The cylinders have diameter D and height H, and are arranged in a continuous matrix material, which we will denote with a subscript "1" when specifying parameters, using the subscript “2" for cylinder parameters. For the materials 1 and 2, we will consider the alternatives of antimony sulphide, air and silica. The grating structure is placed on a silica spacer layer of thickness t, and below this spacer is a silver layer, with thickness 130 nm sufficient to give negligible transmittance in the visible spectral range considered (0.52

Optics EXPRESS

μm to 0.65 μm). For the complex refractive indices of silver, we have used the values from the database Luxpop (www.luxpop.com/), and 1.46 for silica, while for antimony sulphide we have digitised the data from Stürmberg *et al* (see their Fig. S5). The structure is shown schematically in Fig. 1 for the case of the square lattice.

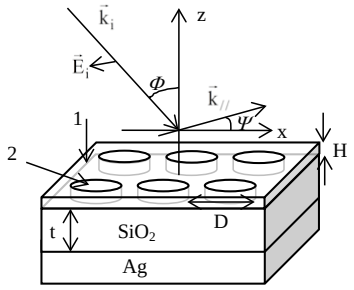

Fig. 1. Schematic representation of the system consisting of a silver substrate, homogeneous layer of SiO_2 with thickness t, and a grating with two-dimensional periodicity (period D in both x and y-directions) and height H which is made of a matrix substance 1 and cylindrical holes made of material 2 (specified in Table 1). The incident direction is specified by two angles, the polar angle ϕ between the incident wavevector and the normal to the surface (z-axis), and the azimuthal angle ψ between the projection $\mathbf{k}_{||}^i$ of $\mathbf{k}^i$ on the xy-plane. The polarization of the incident wave is kept perpendicular to the xz-plane..

In order to calculate the reflection and absorption within the doubly-periodic grating structures, as well as the fields within them, we have employed a rigorous in-house code based on the Fourier Modal Method [17, 18], in conjunction with the Normal Vector Method [19]. All results shown have been verified by convergence studies to be of better than graphical accuracy.

A numerical technique employed in the exploration of the results presented in the next two sections is worth describing. The doubly-periodic gratings investigated are all thin compared with the wavelength, so that their upper and lower surfaces are strongly coupled. A significant number of Fourier terms are needed to accurately model the scattering by such thin gratings, and these are used in all calculations reported here (121, 11 for each direction). This does not mean that all of these terms contribute strongly to the fields reaching the silver mirror. To investigate which plane waves propagating in the silica are important contributors to the field at the mirror and to the resonant phenomena arising between the mirror-grating system, a simple method is to "turn-off" selected plane waves and see the effect on the reflection and absorption by the full structure. This can be done by a post-hoc adjustment of the plane waves in question within the program (after the scattering matrix of the grating layer has been calculated with the full set of plane waves necessary for accuracy), making them so strongly evanescent that their contribution to the mirror-grating coupling is negligible. This mirror-grating coupling involves the interference between the various orders of diffraction generated by the doubly-periodic first layer of the structure, and can affect the absorption within the grating layer in ways which are a priori difficult to predict, for example shifting or splitting absorption peaks.

We have investigated ten different doubly-periodic structures, with common periods $d = 0.375\mu$m along the x and y axes. For each, an optimisation of the values of the cylinder diameter and spacer layer thickness has been made (using steps of 0.5 nm) for several values of the cylinder length, minimising their reflectance at the chosen target wavelength of 0.591 μm. Details of the characteristics of the ten structures and their optical performance are given in Table 1. R is the reflectance at the design wavelength and Φ_{Ag} the flux of the Poynting vector through the top of

Optics EXPRESS

the silver layer. Further discussion of the square grating systems will be given in Section 3, and of the hexagonal systems in Section 4.

Table 1. The parameters of the 10 optimised doubly-periodic absorber systems: lattice type, constituents (1 for the matrix, 2 for the inclusion), spacer thickness, cylinder diameter, cylinder length, reflectance at the design wavelength and flux into the silver substrate. Distances in μm.

system	lattice	1	2	t	D	H	R	Φ_{Ag}
1	sqr	Sb_2S_3	air	0.252	0.247	0.04	$3.5\ 10^{-5}$	2%
2	sqr	air	Sb_2S_3	0.220	0.308	0.04	$6.5\ 10^{-4}$	2.5%
3	sqr	Sb_2S_3	SiO_2	0.192	0.343	0.04	$4.8\ 10^{-4}$	6.2%
4	sqr	Sb_2S_3	SiO_2	0.287	0.280	0.04	$2.1\ 10^{-4}$	2.0 %
5	sqr	SiO_2	Sb_2S_3	0.234	0.322	0.04	$3.4\ 10^{-4}$	1.85%
6	hex	Sb_2S_3	air	0.189	0.107	0.04	2.5 10−4	6.4 %
7	hex	air	Sb_2S_3	0.170	0.263	0.07	$4.0\ 10^{-4}$	4.7%
8	hex	Sb_2S_3	SiO_2	0.173	0.292	0.05	$1.2\ 10^{-3}$	13%
9	hex	Sb_2S_3	SiO_2	0.196	0.154	0.05	7.0 10−4	3.8%
10	hex	SiO_2	Sb_2S_3	0.200	0.307	0.05	1.3 10−4	2.9%

3. Results for the square lattice

In Fig. 2 we show the normal incidence reflectance and absorptance in the silver layer as a function of wavelength, and the angular dependence of reflectance at the wavelength of minimum normal incidence reflectance. In the latter case, the direction of the incident wave is specified in terms of the dimensionless quantities $\alpha = \sin\phi\cos\psi$ and $\beta = \sin\phi\sin\psi$, where ϕ and ψ refer respectively to the polar and azimuthal angles specifying the propagation direction, normal incidence corresponding to $\phi = 0$, and $\psi = 0$ corresponding to a direction of periodicity of the grating. (For guidance, 5° in ϕ then corresponds to $\alpha \approx 0.0873$.).

The reflectance curves of Fig. 2 (left) show the presence of a double minimum, split from the single minimum (black dots) present if only the order $(0,0)$ is allowed to couple the grating with the mirror layer (using the “switching-off" technique described in Section 2). The flux reaching the silver layer maximises at the left reflectance minimum, with a local maximum at the right minimum. The slight glitch in the accurate reflectance curve near 0.56 μm is in fact cause by a discontinuity in the tabulated data for the complex refractive index of silver. The curves of reflectance as a function of incident wave direction in Fig. 2 (right) show that the reflectance begins to rise quickly for a variation of ϕ of about 2.5° away from normal incidence. The curves show the symmetry one expects for this choice of bi-periodic grating (square lattice).

Similar curves for the systems 2-5 whose optimised parameters are given in Table 1 will be found in the Appendix. Note that all five systems considered are capable of giving reflectance minima of essentially zero, but that systems 2 and 3 achieve their minimum with the flux at the silver mirror being significant higher than for systems 1, 4 and 5.

4. Results for the hexagonal lattice

In Fig. 3 we show the reflectance of structure 7 of Table 1 as a function of wavelength. This structure gives reflectance below 20% over the wavelength range from 0.52 μm to 0.60 μm, with two wavelengths of near-zero reflectance (0.555 μm and 0.591 μm). From the blue and red curves, as well as the black points, it is evident that plane wave orders $(0,0)$, $(\pm1,0)$, $(0,\pm1)$ and $\pm1,\pm1)$ in the SiO_2 layer are all significant in generating accurate values for the reflectance.

Optics EXPRESS

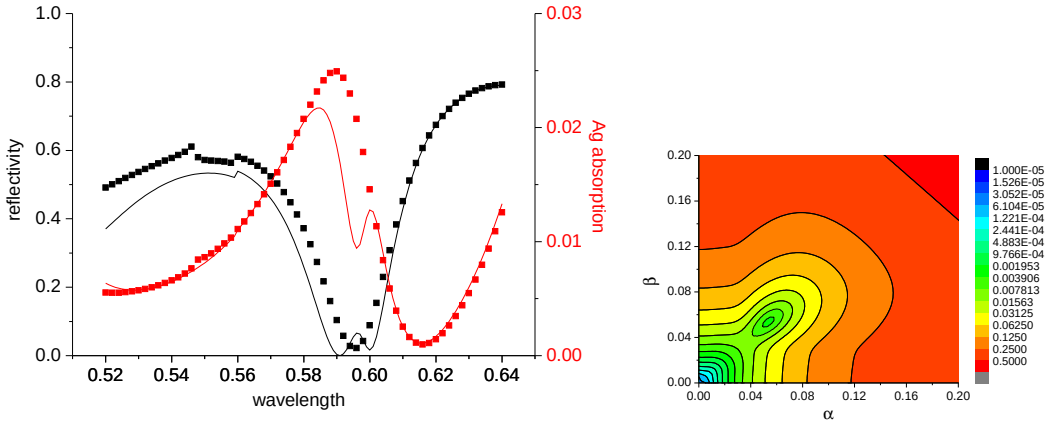

Fig. 2. (Left) Reflectance (black,left scale) and absorptance (red,right scale) in the silver layer of the grating structure of Case 1, Table 1, as a function of wavelength. Full lines - exact values, dots - taking into account the single order $(0,0)$ inside the SiO_2 homogeneous layer. (Right) Reflectance at the wavelength of minimum normal reflectance as a function of dimensionless direction cosines α and β. The electric field of the incident plane wave is along the β axis.

It is interesting that for this case (right curve) the flux absorbed in the silver substrate remains small where the reflectance is small, peaking strongly only after the reflectance minimum at 0.591 μm. The curves below in Fig. 3 show that the process of homogenisation, wherein the doubly-periodic grating is replaced by a layer with an effective permittivity deduced from the equations of electrostatics, is not useful in this case. The technique of homogenisation can only work if it is accurate to neglect the influence of all but the $(0,0)$ order; we have already seen this not to be the case in the upper left part of Fig. 3. The higher order plane waves created by the grating interact significantly with the mirror, and have a strong effect on the amplitude of the $(0,0)$ order reflected beam leaving the structure. (Note that in the comparison made in the lower frame of Fig. 3 the effective permittivity of the plane layer used to replace the grating is obtained using an expression accurate up to 12th order in the volume fraction for the hexagonal array, Eq.(12) in Perrins et al [14].)

The plots of reflectance as a function of direction shown in Fig. 4 exhibit the expected six-fold symmetry of the hexagonal lattice. That at left for a shorter wavelength shows the influence of several modes in its more complex dependence on α and β, whereas that at right for 0.591 μm shows a simple dependence consistent with the accuracy of the results for the $(0,0)$ order alone in Fig. 3 in the upper wavelength range. At 591 nm, the angular dependence is weaker, with the region of reflectivity smaller than 1% covering greater area of the contour diagram (to about 8ą). This weaker dependence is to be expected given the dominant role of the single order $(0,0)$ in this case.

These comments based on reflectance as a function of angle are supported by the maps of scattered field components just above the surface of the bi-periodic grating given in Figs. 5 and 6, and also by the plot of the total field with respect to the coordinate z in the direction normal to the plane in Fig. 7. These field plots just above the grating surface naturally reflect the field structures just within the thin layer, At the shorter wavelength, the different field components have differing structures, reflecting the importance of different modes. For 0.591 μm, there is a single dominant field component (E_x). However, for both wavelengths the strongest fields

Optics EXPRESS

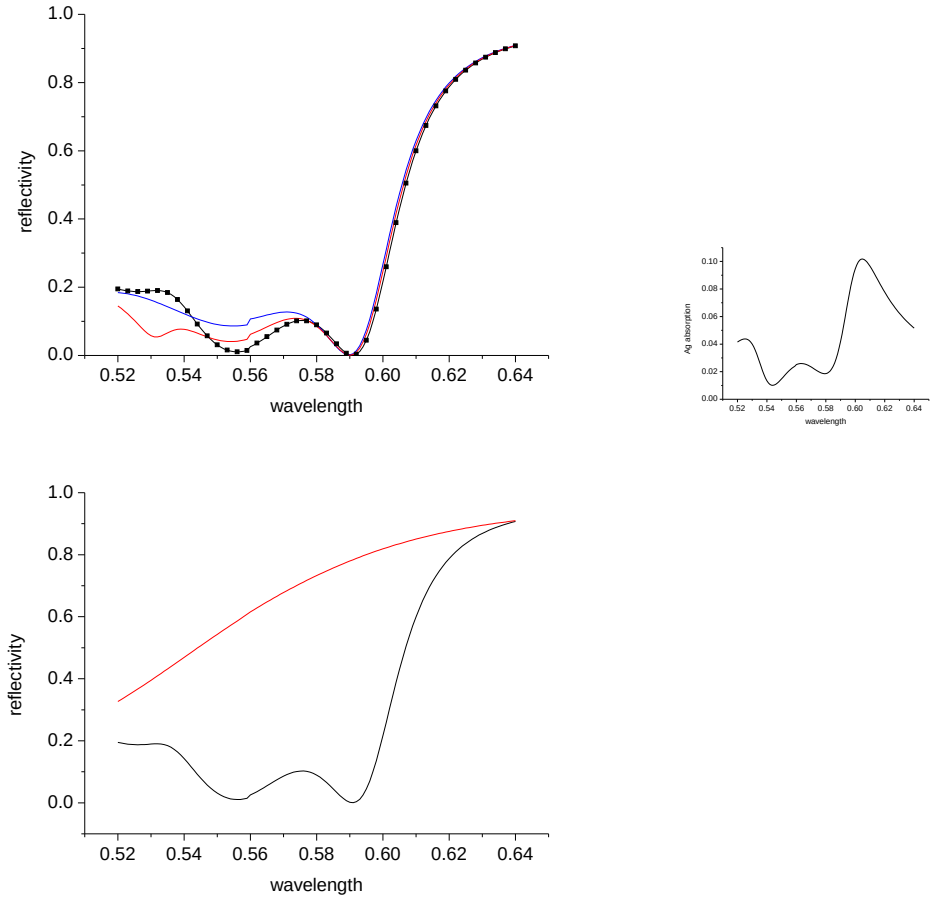

Fig. 3. (Left) Reflectance of the grating structure of Case 7, Table 1, as a function of wavelength: black line, taking into account all diffraction orders in SiO_2, blue curve, only the propagating orders (0,0), red line, orders (0,0), (0,$\pm$1), and ($\pm$1,0), black dots, adding also orders ($\pm$1, $\pm$1). (Right) Flux into the silver substrate as a function of wavelength. Below: Reflectance curve (black) compared with the results of homogenisation (red curve).

occur in within the cylinders (made of antimony sulfide), rather than in the matrix (made of air), and within the grating layer (for z between -0.070 μm to 0) rather than in the silica layer (from -0.240 μm -0.070 μm). Note that in Fig. 7 there is evidence of stronger surface wave effects at 0.5557 μm than at 0.591 μm.

Similar curves for the systems 6,8-10 whose optimised parameters are given in Table 1 will be found in the Appendix. All five hexagonal systems considered are capable of giving reflectance minima of essentially zero, but systems 6 and 8 achieve their minimum with the flux at the silver mirror being significant higher than for systems 7, 9 and 10.

5. Conclusion

We have presented the results of a theoretical study of the absorptance of thin doubly-periodic structures composed of cylindrical inclusions placed on a dielectric spacer, and terminated by a fully-reflecting silver layer. The absorbing material used was the amorphous chalcogenide

Optics EXPRESS

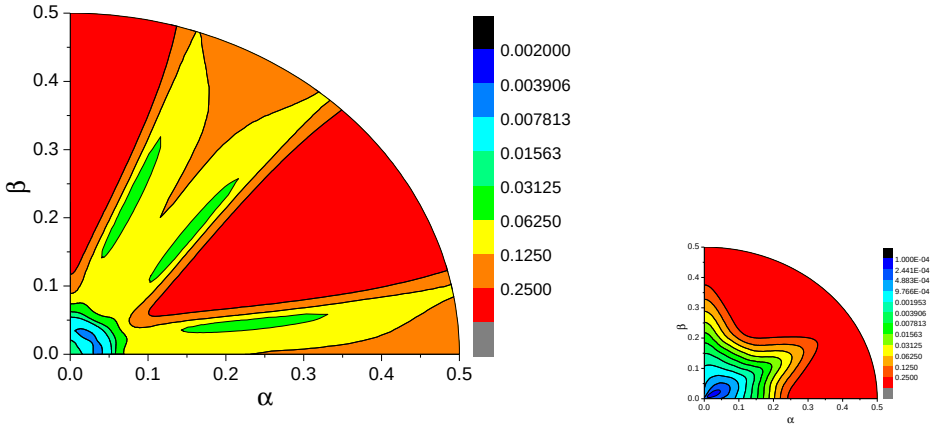

Fig. 4. (Left) Reflectance for the structure of Case 7, Table 1 at a wavelength (0.540 μm) near the first minimum of normal reflectance as a function of dimensionless direction cosines α and β. (Right) As at left, but for the second minimum wavelength (0.591 μm) of normal reflectance.

material antimony sulphide. We have considered both square and triangular lattices of inclusions, both of which generate polarisation-independent absorptance for normally-incident light, and for each lattice we have presented five optimised designs which offer near-perfect absorptance at a chosen wavelength (0.591 μm). Those five designs cover the choices as to whether the antimony sulphide fills the cylinders, or forms the matrix material separating them, and whether the second material in the doubly-periodic layer is the superstrate material (air) or the substrate material (silica). We have shown that the results of rigorous electromagnetic theory calculations are not capable of being well represented by a quasistatic model accurate to the twelfth power of the volume fraction constructed specifically for doubly-periodic arrays of cylinders. We have also shown that the high absorptance arises due to the interaction of the plane wave diffraction orders $(0,0)$, $(\pm1,0)$, $(0,\pm1)$ and $(\pm1,\pm1)$. We have also studied the dependence of absorptance on angles of incidence ranging from 0° to 30°.

The results will be of value in applications of thin absorbers based on chalcogenides and similar weakly-absorbing seminconductors in the visible region. Their experimental validation would be of value, as would their extension to near-infrared wavelengths. This would of course require a determination of optical constants over a wider wavelength range than those reported by Stürmberg et al [15].

6. Appendix

Optics EXPRESS

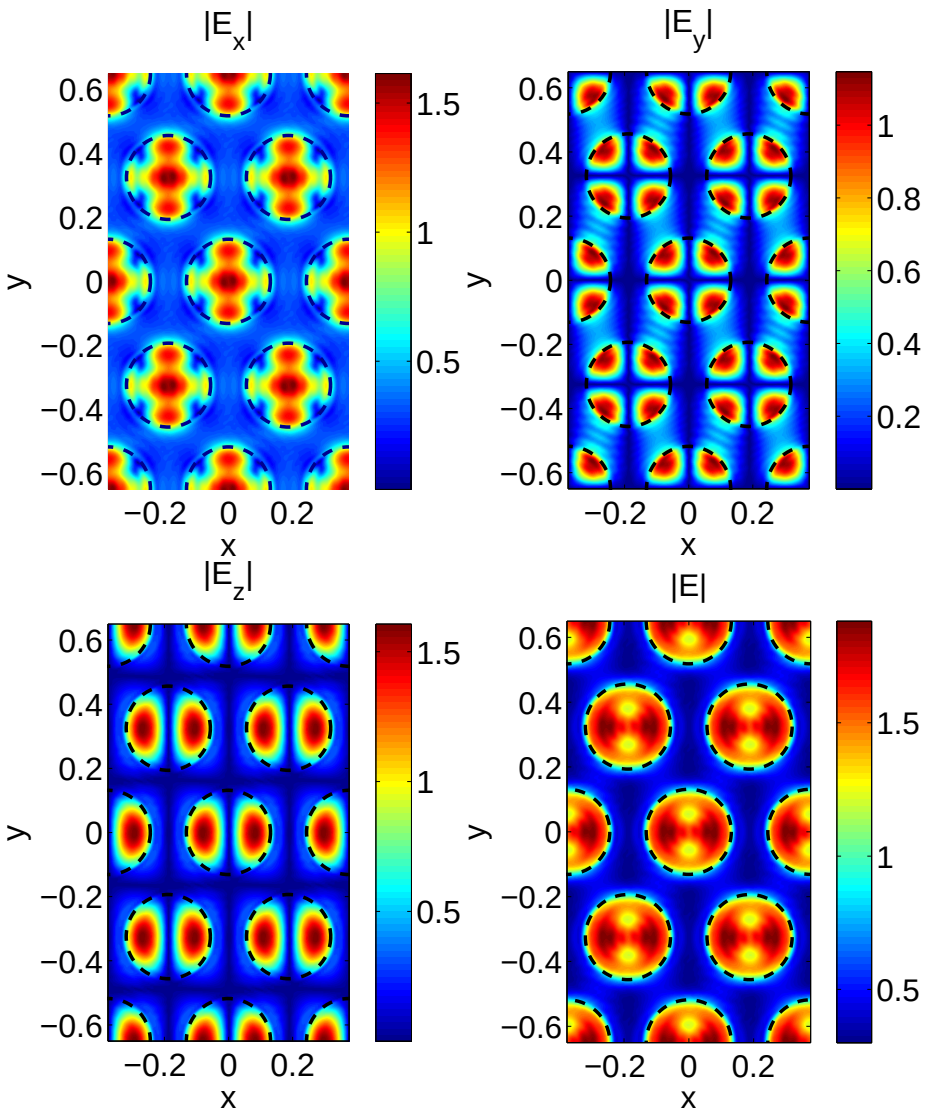

Fig. 5. Scattered field components just above the surface of the biperioidc grating, as a function of position (x, y), for the first minimum wavelength (0.5557 μm) of total reflectance. The black dotted lines represent the cylinders made of antimony sulfide.

Optics EXPRESS

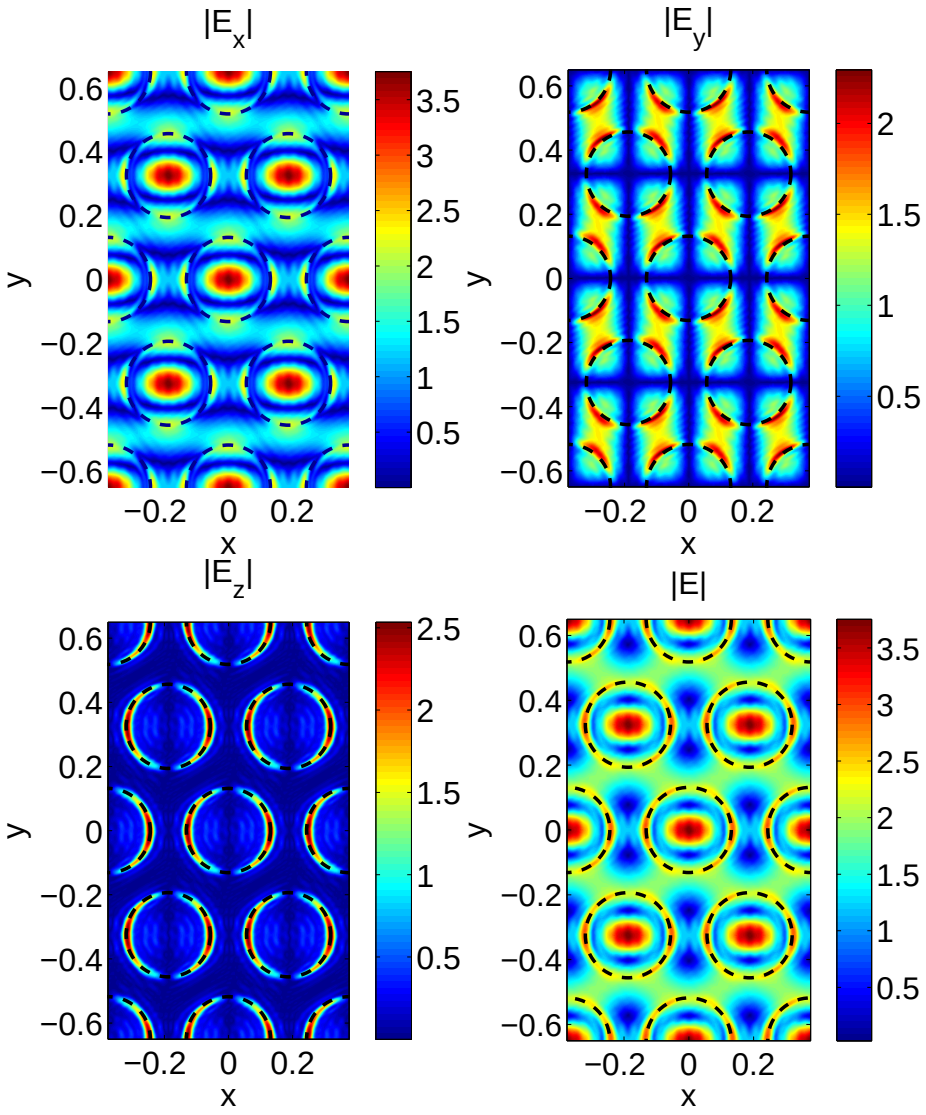

Fig. 6. As for Fig. 5, but for the second minimum wavelength (0.591 μm) of normal reflectance. The incident electric field is along the β axis.

Optics EXPRESS

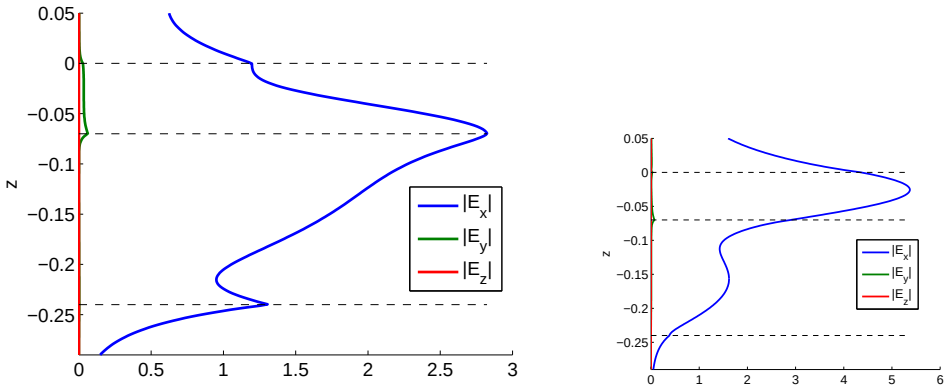

Fig. 7. Total electric field components with respect to z (in μm), in the direction perpendicular to the layers, for $x = y = 0$. (Left) First minimum wavelength (0.5557 μm) of total reflectance. (Right) Second minimum wavelength (0.591 μm) of total reflectance. The black dotted lines represent the layers interfaces from the substrate (bottom) to the superstrate (top).

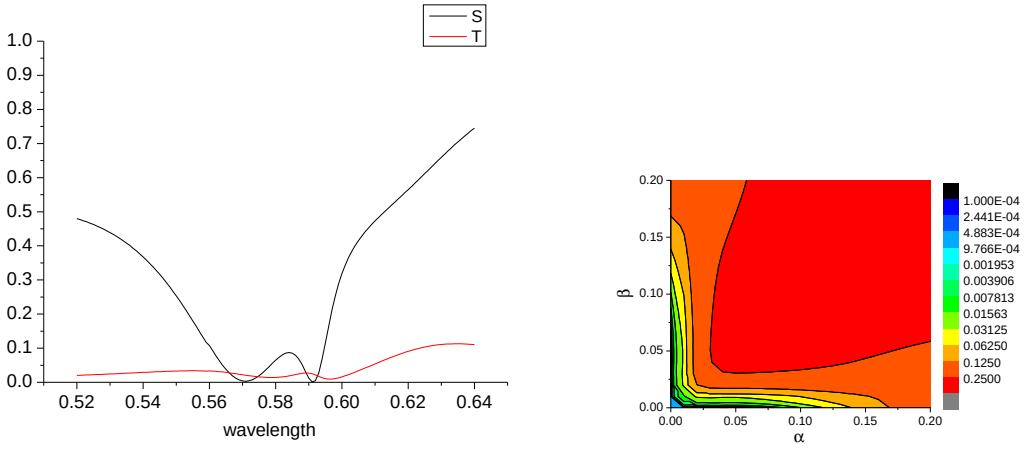

Fig. 8. (Left) Reflectance (black) and absorptance (red) in the silver layer of the grating structure of Case 2, Table 1, as a function of wavelength. (Right) Reflectance at the wavelength of minimum normal reflectance as a function of dimensionless direction cosines α and β.

Optics EXPRESS

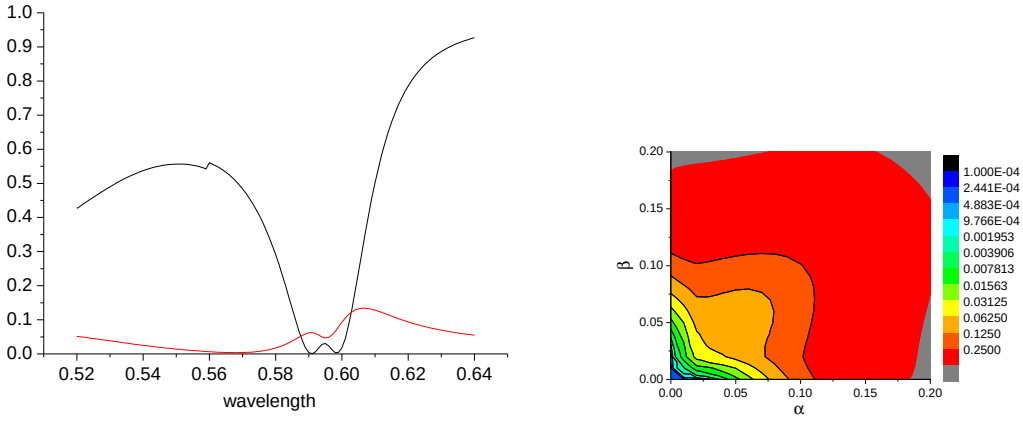

Fig. 9. (Left) Reflectance (black) and absorptance (red) in the silver layer of the grating structure of Case 3, Table 1, as a function of wavelength. (Right) Reflectance at the wavelength of minimum normal reflectance as a function of dimensionless direction cosines α and β.

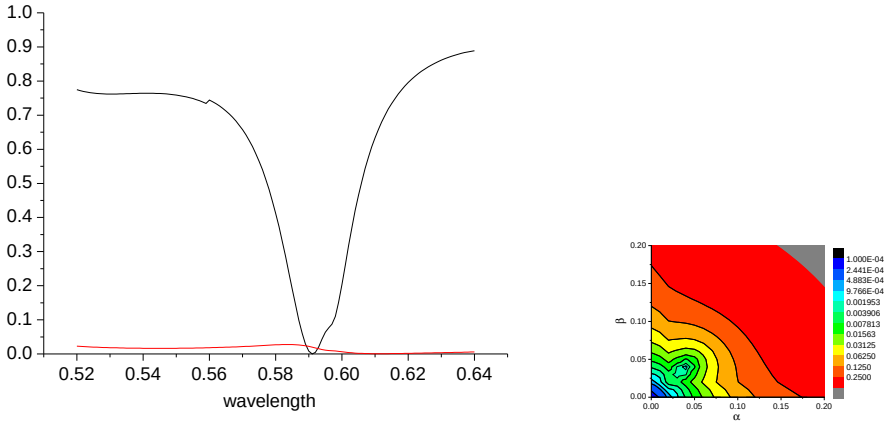

Fig. 10. (Left) Reflectance (black) and absorptance (red) in the silver layer of the grating structure of Case 4, Table 1, as a function of wavelength. (Right) Reflectance at the wavelength of minimum normal reflectance as a function of dimensionless direction cosines α and β.

Optics EXPRESS

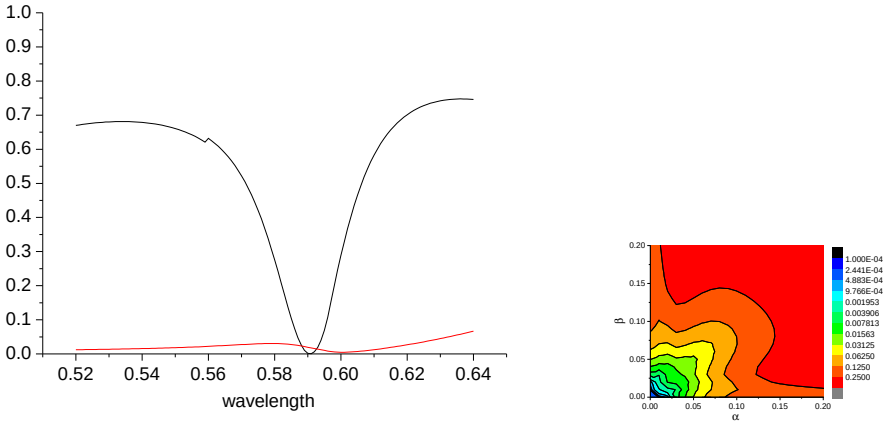

Fig. 11. (Left) Reflectance (black) and absorptance (red) in the silver layer of the grating structure of Case 5, Table 1, as a function of wavelength. (Right) Reflectance at the wavelength of minimum normal reflectance as a function of dimensionless direction cosines α and β.

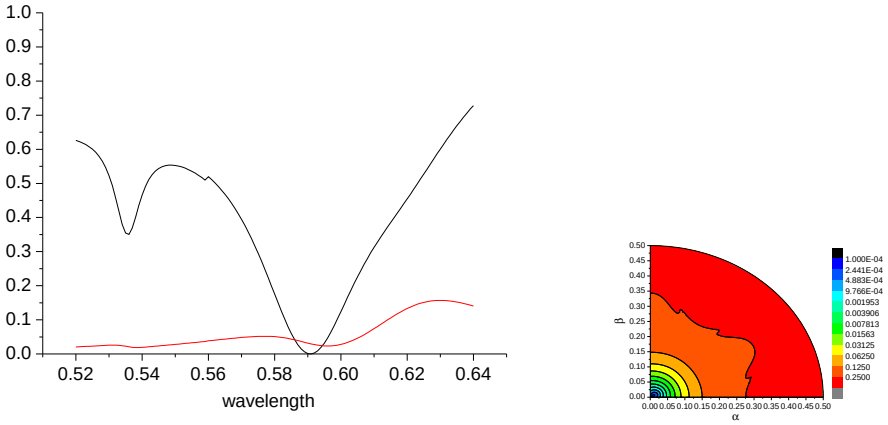

Fig. 12. (Left) Reflectance (black) and absorptance (red) in the silver layer of the grating structure of Case 6, Table 1, as a function of wavelength. (Right) Reflectance at the wavelength of minimum normal reflectance as a function of dimensionless direction cosines α and β.

Optics EXPRESS

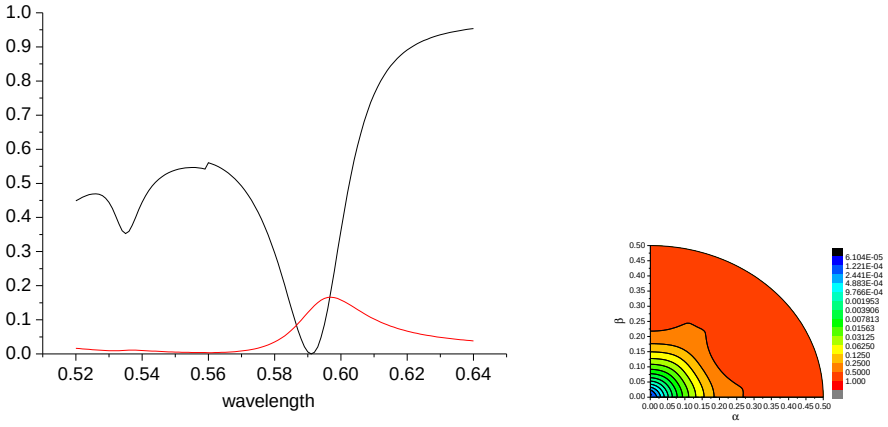

Fig. 13. (Left) Reflectance (black) and absorptance (red) in the silver layer of the grating structure of Case 8, Table 1, as a function of wavelength. (Right) Reflectance at the wavelength of minimum normal reflectance as a function of dimensionless direction cosines α and β.

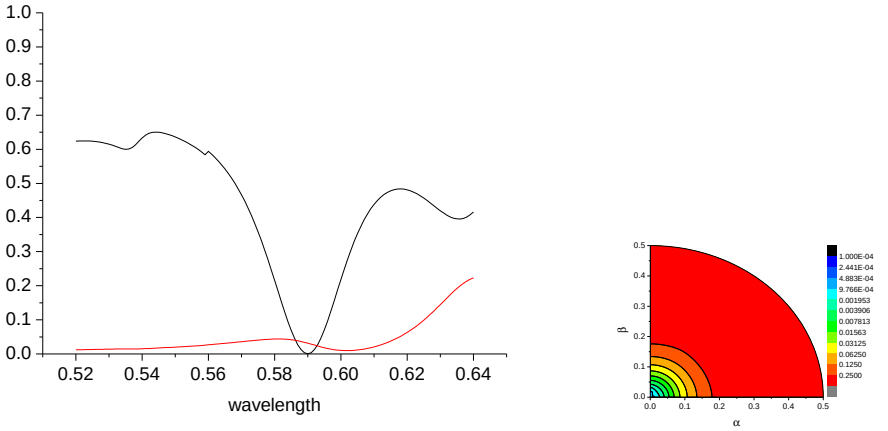

Fig. 14. (Left) Reflectance (black) and absorptance (red) in the silver layer of the grating structure of Case 9, Table 1, as a function of wavelength. (Right) Reflectance at the wavelength of minimum normal reflectance as a function of dimensionless direction cosines α and β.

Optics EXPRESS

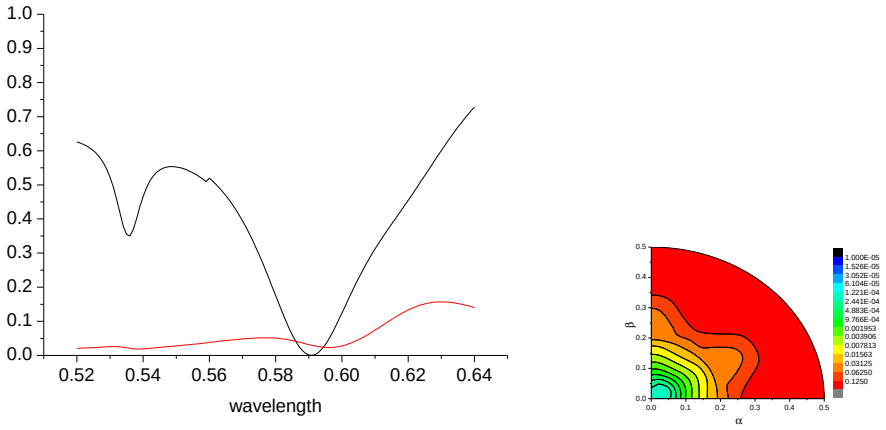

Fig. 15. (Left) Reflectance (black) and absorptance (red) in the silver layer of the grating structure of Case 10, Table 1, as a function of wavelength. (Right) Reflectance at the wavelength of minimum normal reflectance as a function of dimensionless direction cosines α and β.

Acknowledgments

The participation of R. McP. in this work was assisted by the Australian Research Council's Centre of Excellence Scheme CE110001018. Research conducted within the context of the International Associated Laboratory ALPhFA: Associated Laboratory for Photonics between France and Australia. This work has been carried out thanks to the support of the A*MIDEX project (no. ANR-11-IDEX-0001-02) funded by the Investissements d'Avenir French Government program, managed by the French National Research Agency (ANR).